

Nanopatterning mask fabrication by femtosecond laser irradiation

Y. Zhou^a, M.H. Hong^{b,c,*}, J.Y.H. Fuh^a, L. Lu^a, B.S. Luk'yanchuk^b, C.S. Lim^a, Z.B. Wang^b

^a Department of Mechanical Engineering, National University of Singapore, 9 Engineering Drive 1, Singapore 117576, Singapore

^b Data Storage Institute, 5 Engineering Drive 1, Singapore 117608, Singapore

^c Department of Electrical and Computer Engineering, National University of Singapore, 4 Engineering Drive 3, Singapore 117576, Singapore

Abstract

Surface plasmons are photo-coupled quanta of electro excitation at the boundary of a metal and dielectric, which is a charge density wave of free electrons. Another important feature of surface plasmons resonance, in addition to the enhancement of electric field, is the ability to pass through surface structure smaller than incident laser wavelength and makes it have a potential to overcome the diffraction limit resulting in the breakthrough of nanotechnology. For surface plasmon resonance developing a mask with small feature size is vital. In this paper, mask fabrication by laser irradiation on self-assembly silica particles was described. Compared with the theoretical simulation, it is shown that self-assembly particle-assisted nanopatterning can fabricate a mask with very fine features effectively. With a proper particle size, laser wavelength and laser fluence, periodical structures generated can meet the requirement for surface plasmon use.

© 2007 Elsevier B.V. All rights reserved.

Keywords: Laser; Surface plasmon; Nanofabrication; Optical near field; Non-linear absorption

1. Introduction

Surface plasmons, the electron density oscillations near a metal–dielectric boundary surface which was established by Otto [1], provide the method to fabricate sub-wavelength structures for optical devices. Smaller structures require shorter illumination wavelengths. However, it is becoming more difficult and complicated to use the short optical wavelengths to reach the desired feature sizes because the use of wavelength in the deep-ultraviolet requires significantly difficult adjustments [2]. The wavelength of a surface plasmon is much shorter than that of illumination light, so the minimum feature sizes is also much smaller than wavelength which means the parallel light overcoming of diffraction limit. In the surface plasmon theory, the momentum of surface plasmon wave is larger than that of the incident laser. Thus the surface plasmons cannot be excited until that requirement is met. Research shows that the surface plasmons can be excited on air–metal interface with surface metal nanoparticles. The surface plasmon wave will propagate along the substrate surface in terms of evanescent wave

which decays exponentially in the direction perpendicular to the surface. Dimensionally, the wave will be localized within two-dimension surface plane, which is one of the preliminary requirements for optical devices. The future integration of optical devices will require the fabrication of waveguide for surface plasmon wave below the diffraction limit. One of the possibilities is using metal nanoparticles array. The coupling between two adjacent particles builds the coherent energy propagation mode along the array. Even, the light wave turning at the corners of the chain is also possible. This nanoparticle chain shows a high confinement of the electromagnetic energy and allows for highly variable geometries propagation [3].

To further study the propagation properties of surface plasmon wave such as the reflection, focusing and coherence that are still not fully understood, and precisely fabricated metal nanoparticle arrays masks are required. These masks also make possible for new fundamental studies of surface plasmons interactions with periodic structures and novel technologies, including spectroscopically based chemical and biological sensors [4].

Currently, the methods of synthesis of metal nanoparticles are via electrochemical [5], biosynthesis [6], wet chemical [7] and aerosol/vapor-phase routes [8,9]. It is very difficult to arrange these metal nanoparticles as desired only by means of self-assembly. An idea from nanowire presents that nanomaterial can “grow” on pre-designed patterns. Thus topographically modified

* Corresponding author at: Department of Electrical and Computer Engineering, National University of Singapore, 4 Engineering Drive 3, Singapore 117576, Singapore. Tel.: +65 6874 8707; fax: +65 6777 1349.

E-mail address: hong_minghui@dsi.a-star.edu.sg (M.H. Hong).

substrates can be used as templates for ordered array of nanoparticles, by which very well-arranged metal nanoparticles array was obtained through the dewetting of metal thin film [10]. In the reference, metal thin film was first deposited on a patterned silicon wafer. Then the nanoparticle arrays in the silicon patterns will be formed after the sample was annealing in air at 850 °C for 2 h. In that case, the periodical distance and the metal nanoparticles size depend on the pits can be fabricated on the silicon substrate.

For surface plasmons research, however, the substrate should be dielectric, such as glass or quartz. It is, however, a high challenge for glass processing to get nanostructures due to its hard, brittle, nonconductive and other inert properties. It also leads to many investigations on the sophisticated fabrication methods, such as nanoimprinting [11], electron beam lithography [12], and chemical etching. Laser microprocessing is an approach in glass engineering. But the minimum feature size is determined by the diffraction limit of the light. Recently, optical near-field lithography has been developed as a new technology to overcome diffraction limit by self-assembly microspheres [13]. The near-field enhancement due to light scattering by small spherical transparent particle plays an important role. The distribution of laser energy around spherical particles can be calculated from Mie theory. At the interface between particle and glass surface, laser energy is localized within a small region, both inside and outside the particle, with a very high enhancement factor. This highly confined laser energy can locally damage the glass surface and form nanopits.

Femtosecond laser nanomachining is another attractive approach in the glass engineering with the advantages of elimination of collateral damage in dielectrics, reduction of heat-affected zones, and the ability to create limited sub-diffraction target regions. Femtosecond laser can also provide extremely high peak power intensity for non-linear multi-photon absorption. Furthermore, non-linear absorption of femtosecond laser irradiation can result in an increase in the refractive index at the focal point inside the glass, which is potentially effective to produce structures in nanoscale feature size [14]. As simultaneous absorption of n photons is proportional to the n th power of laser fluence, the changes in optical properties can be confined inside a tiny region with its sub-micron dimensions. In this research, nanopits formation by femtosecond laser irradiation on self-assembly microspheres was studied. By depositing a monolayer of microspheres on the substrate surface as a particle mask and utilizing femtosecond laser as a light source, nanoscale pits on the glass surface can be created [15]. It is proposed that non-linear absorption and optical near-field enhancement play the important roles in the nanopit formation on the glass substrate.

2. Experimental

Glass substrate was cleaned with acetone in an ultrasonic bath for 15 min followed by rinsing in IPA and DI water for 5 min, respectively and then dried by N₂ gas (purity 99.999%). The spherical silica particles (Duke, $n = 1.6$, 10% size deviation) with the diameter of 1 μm were applied on the glass substrate after the suspension had been diluted with DI water. The substrate was kept still until all the water had been evaporated. As a result, a silica monolayer array was formed on the substrate surface.

A Ti:Sapphire (Spectra Physics Tsunami, Mode 3960) and a regenerative amplifier (Spectra Physics Spitfire, Mode 9769A) were used as the light source (wavelength, $\lambda = 800$ nm, pulse duration, $\tau = 100$ fs and repetition rate from 1 to 1000 Hz). The laser coming out from the aperture was reflected by mirrors and then focused by a 20 \times microscope objective lens mounted on a Z stage. The laser spot size is about 5.4 μm . The laser fluence is in the range from 17.5 to 52.5 J/cm². The laser was incident normal to the substrate surface. After the exposure the sample was characterized by AFM (Digital Instruments D3000) and FESEM (Hitachi S-4100). For SEM imaging samples were coated with a thin Au film by thermal evaporator before observation.

3. Results and discussion

Fig. 1 shows a typical nanopits array created on the glass substrate after single femtosecond laser shot at a laser fluence of 17.5 J/cm². As it can be seen, the silica particles on glass surface were removed after the laser irradiation, and nanostructures were formed at the place where the particles originally were located. It is hard to be removed by the conventional ultrasonic cleaning method due to the strong adhesion. The size of nanopit was measured by AFM and found with 150 nm in diameter and 150 nm in depth. The ratio of depth to width is 1:1. It was observed that the edges of these nanostructures are free of cracks. This can be contributed to the ultrashort laser pulse. For long pulse duration laser the formation of cracks was mainly caused by laser associated high temperatures and high pressure [16]. Processing with ultrashort laser pulses essentially eliminates the heat flow to the surrounding material. Therefore, thermally induced substrate cracking is prevented.

To further investigate the influence of laser fluence on the formation of nanopits, the experiments with different laser fluences were repeated. Fig. 2 shows the SEM image of nanopatterns on a glass surface by laser irradiation on the particle mask at a laser fluence of 43.8 J/cm² and the definition of nanopits and melting zone. The size of nanopits and melting zone are obviously larger than those formed at a lower laser fluence. Meanwhile, debris was observed around the nanopits. Fig. 3 is the relationship between the average sizes of the nanopits and the melting zone as functions of laser fluence with five measurements accordingly. From these figures, both nanopits and melting zone sizes

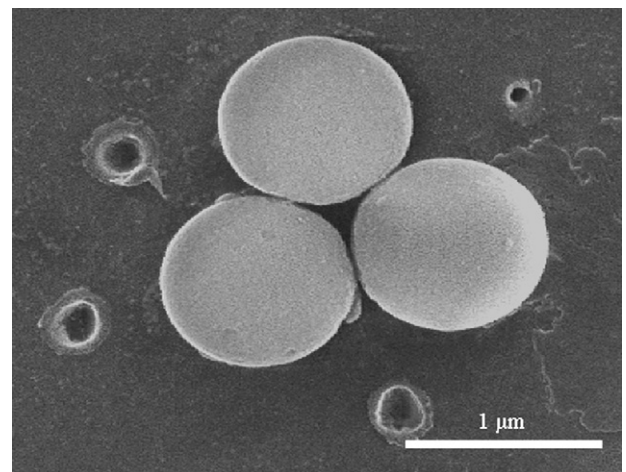


Fig. 1. SEM image of nanopits formed under 1.0 μm silica particles on glass surface by 800 nm, 100 fs laser pulse irradiation at a laser fluence of 17.5 J/cm².

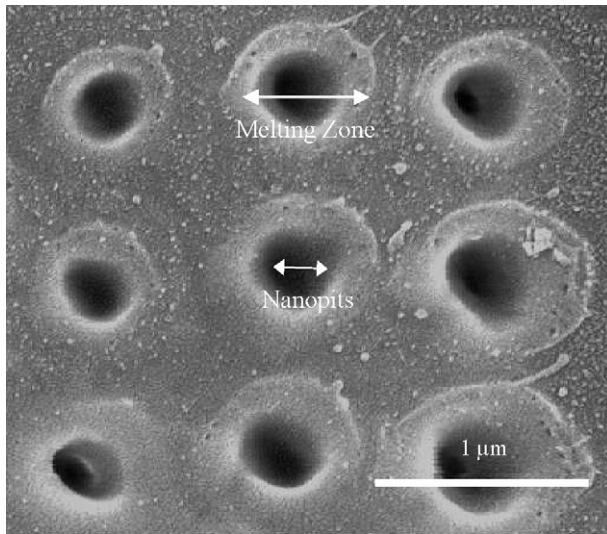


Fig. 2. SEM image of the patterns on the glass substrate after the laser irradiation at a laser fluence of 43.8 J/cm^2 .

increase with the laser fluence but the melting zone increases faster than the nanopits. At a high laser fluence, the melting zone can be as large as the particle size of $1 \mu\text{m}$. While the diameter of the nanopits remains at about 300 nm . And the depth of the nanopits measured by AFM also remains at around 150 nm due to the high transparency and low total laser energy input. In contrast, glass substrate without particle mask was irradiated at the same laser fluence. No damage was observed. It shows that particle-assisted near-field enhancement is the main mechanism for the formation of nanopits.

In order to explain the formation of nanopits, the interaction between an ultrashort laser and transparent glass materials has to be analyzed. Since glass is transparent to 800 nm wavelength, the nanopits could not be created with long pulse duration laser irradiation at that wavelength. Electrons absorb photon energy and consequently transfer the energy to lattices in a very short time that is generally in the timescale of several tens of picoseconds [17] in the condition of long pulse exposure. However multiphoton absorption often takes place for the femtosecond laser pulse interaction with glass. The n -photon absorption is propor-

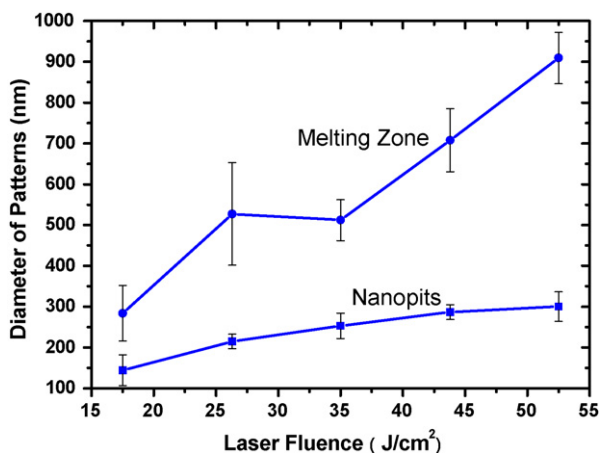


Fig. 3. Average sizes of nanopits as functions of laser fluence.

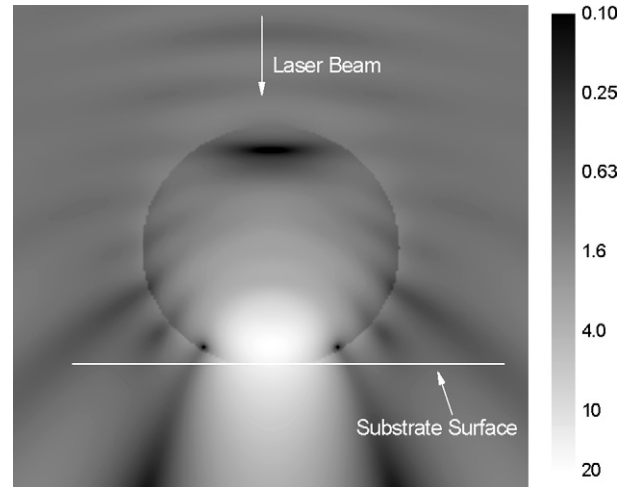


Fig. 4. Contour plot of calculated laser energy distribution, $S_z = III_0$, within incident plane under a $1.0 \mu\text{m}$ silica particle, where laser is irradiated normally on the particle and the refractive index of particle is 1.6.

tional to the n th power of the intensity. This effect significantly narrows the processed area. As a result, with femtosecond laser, the processing area should be confined in the central part of the optical axis [18]. Furthermore, femtosecond laser-induced nonlinear effect gives rise to the change of glass optical properties affecting the propagation of incident light. Then the laser beam was self-focused in a small area and extremely high laser fluence generated nanoscale feature on glass.

Besides the above effects, the near-field enhancement due to light scattering by the small spherical transparent particle plays an important role as well. The distribution of laser intensity on the surface of glass under the spherical particle can be found from the particle on surface theory. We used a fast algorithm of reflected matrix calculation, suggested in Ref. [19]. In Fig. 4 the normalized distribution of the z -component of the Poynting vector (optical enhancement $S_z = III_0$) is shown by taking the spherical center as an original point, laser propagation direction as z -axis. Here I_0 is the input laser intensity. Parameters which were used in calculations correspond to the experiment: particle diameter $2a = 1 \mu\text{m}$, laser wavelength $\lambda = 800 \text{ nm}$ and refraction index for particle and glass $n = 1.6$. One can see from Fig. 4 that maximum laser intensity is localized within a small region of about 350 nm . Because of the ultrashort pulse duration, the final size of nanopits could be smaller than simulation result without considering pulse duration parameter. Around this central zone, high order enhancement is also shown in the simulation, which will modify the pit's shape. In the previous work, tri-hole structure was observed [20]. The modification of the pit shape can be qualitatively understood considering some threshold intensity $I > I_{tr}$ necessary to produce the hole structure. In experiment the whole region was destroyed at high fluences. However formation of the ring around the central hole was found in experiments with film of phase-change material. Pattern of the intensity distribution under the particle was discussed previously in Refs. [21,22]. By tuning the laser input intensity precisely, pits smaller than 100 nm can be formed, which is only one eighth of laser wavelength.

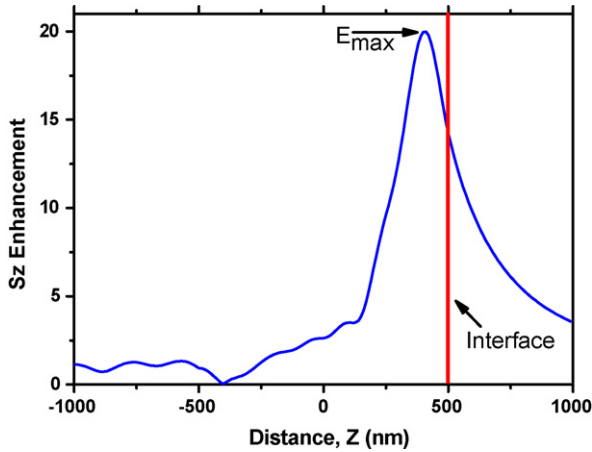


Fig. 5. Normalized poyniting intensity distribution along z -axis under a silica particle ($a=0.5\ \mu\text{m}$) by 800 nm femtosecond laser irradiation based on Mie theory.

As for the debris formation, some of them were resulted from the broken silica particles on the substrate. Fig. 5 is the normalized poyniting intensity distribution along z -axis under a silica particle ($a=0.5\ \mu\text{m}$, $n=1.6$) by 800 nm femtosecond laser irradiation. It indicates that the maximum enhancement point, E_{max} , is located inside the particle. Hence, if nanopits can be formed on glass substrate surface, the laser intensity inside the silica particle is definitely larger than the damage threshold. Then during the laser irradiation, the particle exploded into pieces. Hence, some of the ablation debris comes from the exploded silica particles due to that highly localized field inside the sphere. After trying to prevent the pattern from debris by changing defocus distance, no improvement was obtained. Another way to reduce the debris is to use bigger particles. Fig. 6 is the normalized poyniting intensity distribution along z -axis under a silica particle ($a=3.42\ \mu\text{m}$, $n=1.6$) by 800 nm femtosecond laser irradiation. The focus point was found at the interface between particle and substrate surface. And the intensity enhancement decreases abruptly which makes the particle possible to survive after laser illumination. Fig. 7 presents the

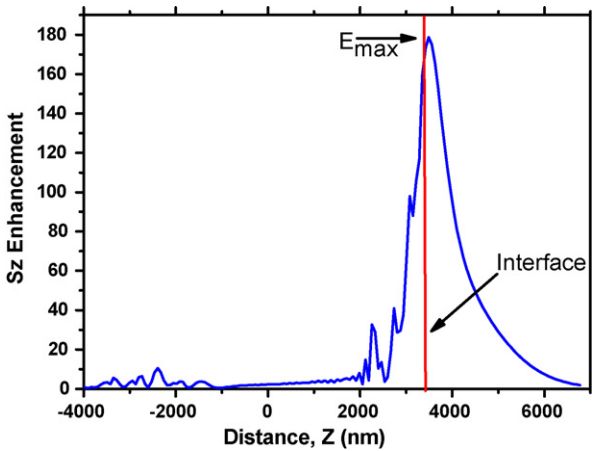


Fig. 6. Normalized poyniting intensity distribution along z -axis under a silica particle ($a=3.42\ \mu\text{m}$) by 800 nm femtosecond laser irradiation based on Mie theory.

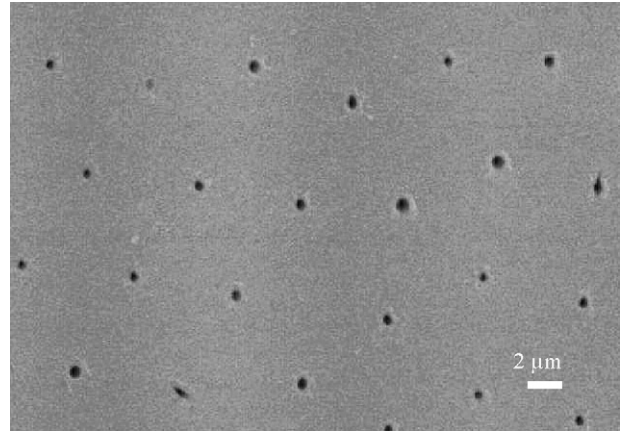


Fig. 7. SEM images of substrate surface after femtosecond laser (100 fs, 800 nm) irradiation of self-assembly $6.84\ \mu\text{m}$ silica particles.

image of substrate surface after the 800 nm femtosecond laser irradiation on $6.84\ \mu\text{m}$ diameter silica particles. Few debris was found. The nanopits formed hexagonally closed-packed array on the glass surface with the diameter of 400 nm which is half of the incident laser wavelength—diffraction limit.

Naturally, the nanopits size depends on the particle diameter if the input laser fluence remains the same. The calculations of enhancement area size of full widths at half maximum (FWHM) and different laser wavelength are shown in Fig. 8 with the particle diameters of 1, 2, 4, 6, 8 and 10 μm, respectively. It was found that for 1 and 2 μm particles, the FWHM sizes increase with incident laser wavelength. For other size particles, such relation cannot be observed. While, FWHM size jumping-up exists for all particles. This is due to the second order enhancement zone which can significantly enlarge the FWHM size. Increasing particle diameter further, the second order enhancement occupies much more laser energy resulting in the energy decreasing of first order enhancement zone or in other words, the first order enhancement zone was compressed. Then the FWHM size is shrunk pronouncedly. The jumping point moves right when laser wavelength increases which means that for longer wavelength the range of particle diameters for stable enhancement zone size

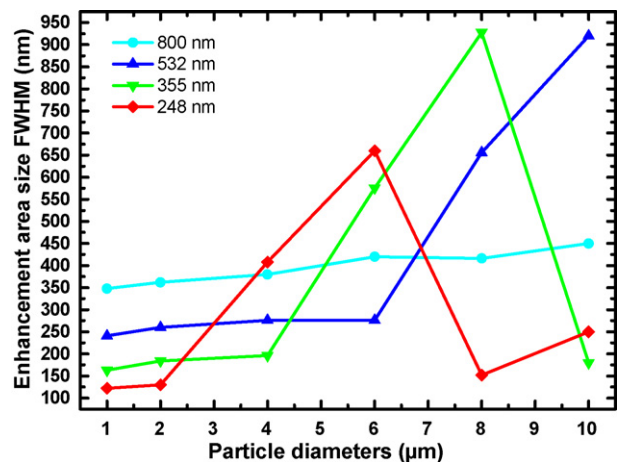


Fig. 8. The FWHM size of enhancement zone with different particle sizes on the substrate surface.

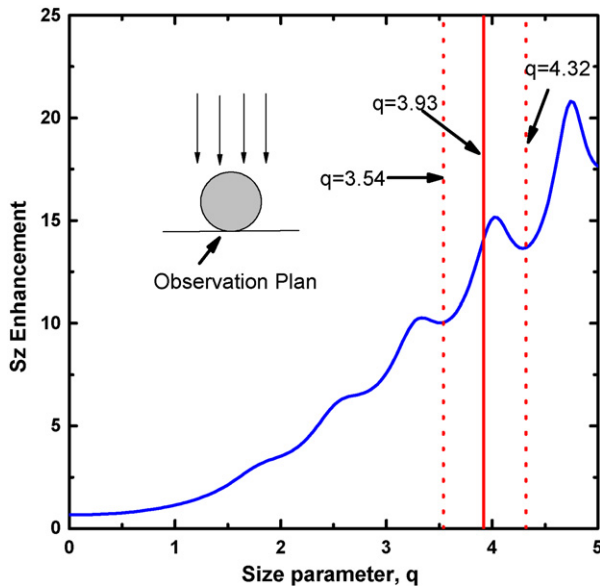


Fig. 9. Variation of the optical near-field enhancement under the particle as a function of particle size. The silica particle is considered as a non-absorbing material of the laser light with a refractive index of 1.6.

is wider than near ultraviolet laser. Hence in the industry applications, to improve the size uniformity, red or near infrared lasers are to be employed.

The enhancement is sensitive to the particle size and incident laser wavelength. A size parameter $q = 2\pi a/\lambda$ is defined. Small variations in size parameter can lead to big variations in enhancement intensity. The silica particles used in the experiments have a size deviation of 10%, which corresponds to a variation in size parameter q from 3.54 to 4.32. Fig. 9 presents the optical near-field enhancement as a function of q . As it can be seen, the enhancement is about 10 times for $q = 3.54$ ($2a = 902$ nm) while 15 times for $q = 4.12$ ($2a = 1050$ nm), which shows an oscillation. It can be clearly seen in Fig. 10, where size variation in the nanopits was bigger than 30% although variation of the particle size was smaller than 10% because the difference in the enhancement factor strongly affects the formation of nanopits under the same laser fluence irradiation.

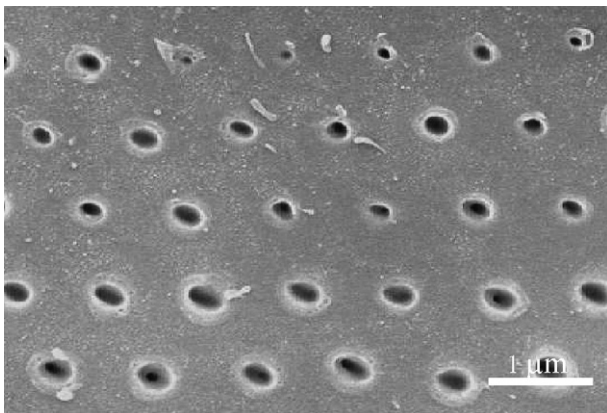


Fig. 10. The nanopit sizes variation.

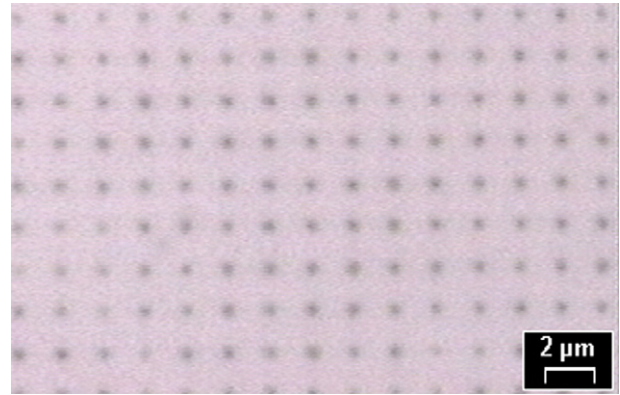


Fig. 11. Pits matrix by 1 μm spherical lens array.

Actually, the calculation shows that even using 10 μm diameter particle, the enhancement laser energy will still be confined in an area with only 450 nm diameter. This technique has a potential to be applied to nanomachining on transparent material in optical near field with tens of micrometers lens. For large area patterns, 1 μm diameter spherical lens array on quartz through which nanopits array were demonstrated by 248 nm laser irradiation as shown in Fig. 11. After mounting the microlens array on a CNC stage, complicated sub-micro structures on transparent materials are feasible.

4. Conclusions

In summary, nanopits were created on the glass surface by 800 nm femtosecond laser irradiation of self-assembled 1 μm silica particles mask. No cracks were found at edges of produced nanostructures on the glass surface. The feature sizes were found from 150 to 300 nm with the average depth of 150 nm. Nanopits formation can be attributed to two main reasons: (1) non-linear effect arising from the interaction of femtosecond laser pulse with transparent glass substrate, and (2) optical near-field enhancement due to light scattering by the transparent silica particles. Self-assembly particle assistant mask fabrication can draw the surface plasmon research more attention. Silica micro particles can be used to generate nanopits to control the dewetting of thin film for ordered metal nanoparticles. Through spherical micro lens array, even bigger size spherical lens can be employed to fabricate sub-micron feature size structure in transparent material.

References

- [1] A. Otto, Z. Phys. 216 (1968) 398.
- [2] X.G. Luo, T. Ishihara, Opt. Express 14 (2004) 3055–3065.
- [3] S.A. Maier, M.L. Brongersma, P.G. Kik, S. Meltzer, A.A.G. Requicha, A. Atwater, Adv. Mater. 13 (2001) 1501–1505.
- [4] E. Kwak, J. Henzie, S.H. Chang, S.K. Gray, G.C. Schatz, T.W. Odom, Nanoletters 5 (2005) 1963–1967.
- [5] H. Thomas, Z. Michael, S. Andrey, S. Joachim, W. Dieter, S.W. Otto, V.M. Vladimir, Angew. Chem. Int. 44 (2005) 6775–6778.
- [6] M. Sastry, A. Ahmad, M.I. Khan, R. Kumar, Curr. Sci. 2 (2003) 162–170.
- [7] M.L. Lius, Mater. Today 2 (2004) 26–31.
- [8] M. Rajala, K. Janka, P. Kykkanen, Rev. Adv. Mater. Sci. 5 (2003) 493–497.

- [9] M.T. Swihart, *Curr. Opin. Colloid Interf. Sci.* 8 (2003) 127–133.
- [10] L. Giermann, C.V. Thompson, *Appl. Phys. Lett.* 86 (2005) 121903.
- [11] S.Y. Chou, P.R. Krauss, P.J. Renstrom, *J. Vac. Sci. Technol. B* 14 (1996) 4129–4133.
- [12] J.R. Wendt, G.A. Vawter, R.E. Smith, M.E. Warren, *J. Vac. Sci. Technol. B* 13 (1995) 2705–2708.
- [13] H. Schmid, H. Biebuyck, B. Michel, *Appl. Phys. Lett.* 72 (1998) 2379–2381.
- [14] S. Theppakuttai, S.C. Chen, *Appl. Phys. Lett.* 83 (2003) 758–760.
- [15] S.M. Huang, M.H. Hong, B.S. Luk'yanchuk, Y.W. Zheng, W.D. Song, Y.F. Lu, T.C. Chong, *J. Appl. Phys.* 92 (2002) 2495–2498.
- [16] Y. Kanemitsu, Y. Tanaka, *J. Appl. Phys.* 62 (1987) 1208–1211.
- [17] S.I. Anisimov, B.S. Luk'yanchuk, *Physics Uspekhi* 45 (2002) 293–296.
- [18] K. Piglmayer, R. Denk, D. Bäuerle, *Appl. Phys. Lett.* 80 (2002) 4693–4695.
- [19] Z.B. Wang, M.H. Hong, B.S. Luk'yanchuk, Y. Lin, O.F. Wang, T.C. Chong, *J. Appl. Phys.* 96 (2004) 6845–6850.
- [20] Y. Zhou, M.H. Hong, F.Y.H. Jerry, L. Lu, B.S. Luk'yanchuk, Z.B. Wang, L.P. Shi, T.C. Chong, *Appl. Phys. Lett.* 88 (2006) 023110.
- [21] B.S. Luk'yanchuk, N. Arnold, S.M. Huang, Z.B. Wang, M.H. Hong, *Appl. Phys. A* 77 (2003) 209–213.
- [22] B.S. Luk'yanchuk, Z.B. Wang, W.D. Song, M.H. Hong, *Appl. Phys. A* 79 (2004) 747–750.